Published online 10 December 2008

Nucleic Acids Research, 2009, Vol. 37, No. 2 ***611–621***
doi:10.1093/nar/gkn977

Molecular recognition of poly(A) by small ligands: an alternative method of analysis reveals nanomolar, cooperative and shape-selective binding

Özgül Persil Çetinkol and Nicholas V. Hud*

School of Chemistry and Biochemistry, Parker H. Petit Institute of Bioengineering and Bioscience, Georgia Institute of Technology, Atlanta, GA 30332-0400, USA

Received October 21, 2008; Revised November 18, 2008; Accepted November 19, 2008

ABSTRACT

A few drug-like molecules have recently been found to bind poly(A) and induce a stable secondary structure ($T_m \approx 60^\circ C$), even though this RNA homopolymer is single-stranded in the absence of a ligand. Here, we report results from experiments specifically designed to explore the association of small molecules with poly(A). We demonstrate that coralyne, the first small molecule discovered to bind poly(dA), binds with unexpectedly high affinity ($K_a > 10^7\ M^{-1}$), and that the crescent shape of coralyne appears necessary for poly(A) binding. We also show that the binding of similar ligands to poly(A) can be highly cooperative. For one particular ligand, at least six ligand molecules are required to stabilize the poly(A) self-structure at room temperature. This highly cooperative binding produces very sharp transitions between unstructured and structured poly(A) as a function of ligand concentration. Given the fact that junctions between Watson–Crick and A·A duplexes are tolerated, we propose that poly(A) sequence elements and appropriate ligands could be used to reversibly drive transitions in DNA and RNA-based molecular structures by simply diluting/concentrating a sample about the poly(A)-ligand 'critical concentration'. The ligands described here may also find biological or medicinal applications, owing to the 3′-polyadenylation of mRNA in living cells.

INTRODUCTION

The polymorphism of DNA and RNA *in vivo* presents numerous opportunities for new therapeutic agents. Accordingly, the design of small molecules that bind noncanonical nucleic acid structures (i.e. non-B- and A-form structures) represents an active area of rational drug design (1–6). Nucleic acids have also emerged as the material of choice for the creation of supramolecular assemblies in nanotechnology and, as we have recently discussed, small molecule-DNA interactions represent another dimension for expanding the functionality and dynamics of DNA-based nanotechnology (7–11).

Among the single stranded nucleic acids, poly(A) is of particular biological relevance due to its role in gene expression. Poly(A) tails, synthesized by poly(A) polymerase (PAP), are found at the 3′-end of mRNAs. These polyadenylate tails are important factors that contribute to the stability and maturation of mRNA, as well as the initiation of translation (12,13). Since the discovery that Neo-PAP (a human PAP), is overexpressed in some human cancer cells (14,15), it has been suggested that the poly(A) tails of mRNA may represent a malignancy-specific target (16).

At present, only four molecules have been reported to bind poly(A) with high affinity and good selectivity over Watson–Crick duplexes (Figure 1) (16–19). These four molecules have similar overall structures. Each has four fused six-membered rings, with a crescent shape and larger surface area than the tricyclic planar molecules typically found to intercalate DNA and RNA duplexes (e.g. the acridines and phenanthridines). Similar to the common acridinium and phenanthridinium ligands, the four reported poly(A) binders have electron-donating substituents. Coralyne and palmatine have methoxy groups attached at different positions, while berberine and sanguinarine have methylenedioxy groups that form five-membered rings at the ends of their extended ring systems.

Coralyne and sanguinarine have been demonstrated to induce the formation of a poly(A) self-structure upon binding (16,19). This self-structure has been suggested to be very similar to the coralyne-induced self-structure of poly(dA), a structure that is most stable around neutral

*To whom correspondence should be addressed. Tel: +1 404 385 1162; Fax: +1 404 894 2295; Email: hud@chemistry.gatech.edu

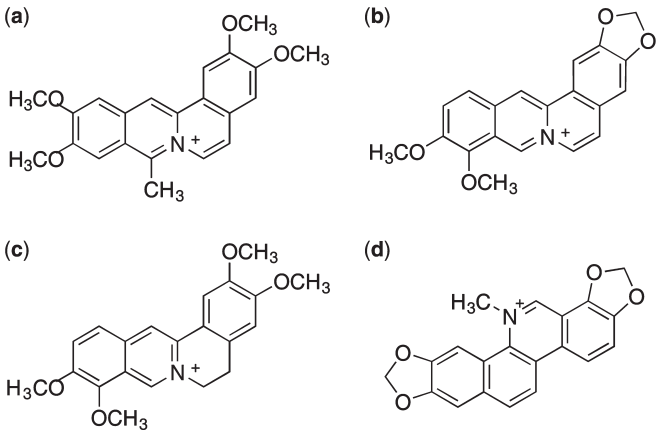

Figure 1. Chemical structures of (**a**) coralyne (**b**) berberine (**c**) palmatine (**d**) sanguinarine.

pH (16). We initially demonstrated that the poly(dA) self-structure is an anti-parallel duplex with ostensible A·A base pairs that is distinct from the previously reported parallel-stranded, hemi-protonated poly(A) duplex that is most stable under slightly acidic conditions (20).

Here, we report investigations into the structural characteristics of poly(A) ligands. We provide evidence that size and a crescent shape are important features of small molecules that induce and stabilize the poly(A) self-structure. Our studies demonstrate that minor structural changes in a ligand can result in tremendous changes in binding affinity for poly(A). Furthermore, our investigations reveal that, because of the rigorous and cooperative ligand dependence, the behavior of ligand-driven assembly of the poly(A) self-structure is such that classical approaches for analyzing ligand–nucleic acid interactions can over- or underestimate the binding constants of some molecules. In particular, we report that the association constant of coralyne for poly(A) is higher than previously appreciated and among the highest reported for any small molecule that binds to a nucleic acid double helix with stoichiometry and spectral characteristics consistent with intercalation. Our analysis of the binding of molecules with lower affinity than coralyne demonstrate the cooperative ligand dependence of the poly(A) self-structure, a system that is physically similar to micelle formation, as described by the critical micelle concentration (CMC) model (21–24). The method used for making such measurements and that used for data analysis could prove useful for a wider range of nucleic acid systems in which ligand binding is a necessary condition for secondary structure formation.

MATERIALS AND METHODS

Materials

The concentrations of stock solutions for berberine chloride and coralyne chloride (Sigma) in H_2O were determined spectrophotometrically using the extinction coefficients: berberine $\varepsilon_{344} = 22500\,M^{-1}\,cm^{-1}$; coralyne $\varepsilon_{420} = 14500\,M^{-1}\,cm^{-1}$. The ellipticine (EMD Biosciences Inc) stock solution was prepared in DMSO, with the concentration determined using $\varepsilon_{295} = 60000\,M^{-1}\,cm^{-1}$. Aza3-5 were synthesized as described previously (25–27). Aza3-5 stocks were also prepared in DMSO and concentrations were determined using the extinction coefficients; aza3 $\varepsilon_{343} = 47\,700\,M^{-1}\,cm^{-1}$; aza4 $\varepsilon_{387} = 32\,100\,M^{-1}\,cm^{-1}$; aza5 $\varepsilon_{407} = 32\,000\,M^{-1}\,cm^{-1}$. The extinction coefficient $\varepsilon_{258} = 9800\,M^{-1}\,cm^{-1}$ nucleotide^{-1} was used for poly(A) (Sigma). All samples were prepared in 1 × BPE (6 mM Na_2HPO_4, 2 mM NaH_2PO_4 and 1 mM Na_2EDTA) with 20 mM NaCl at pH 7.0 (also the buffer for dilution experiments).

Circular Dichroism

Circular Dichroism (CD) spectra were acquired on a JASCO J-810 CD spectropolarimeter equipped with Peltier temperature control unit. Spectra were acquired using either a 0.5 or 1 cm path length cell. CD melting profiles were acquired from 5°C to 80°C or 95°C with 5°C steps, with all samples 60 μM in nucleotide base and 15 μM in small molecule. For determination of T_m values, the intensity of induced long-wavelength CD bands were monitored as a function of temperature. All resulting melting curves were monophasic, and no cooperative melts were observed for poly(A) in the absence of a small molecule ligand.

Job plot analyses were carried out at 5°C, with [ligand] and [poly(A)]/4 fixed at 15 μM (28). The CD intensity at 245 nm was normalized with respect to poly(A) concentration. For pH dependence experiments, samples were prepared in the standard buffer and adjusted with 1 M HCl.

UV–vis spectroscopy

UV–vis absorbance measurements were performed using a HP 8453 UV–vis diode array spectrophotometer equipped with an Agilent 89090A Peltier temperature control unit. For dilution experiments, nearest-neighbor ligand-poly(A) samples, 200 μM in nucleotide and 50 μM in ligand, were prepared in the standard buffer. These samples were diluted with buffer to the desired concentration, and spectra were collected after each dilution, all at room temperature. For high concentrations, a 1 cm path length cell was used, and for low concentrations (<10 μM in nucleotide), a 10 cm path length cell was used. Additionally, spectral integration times of 10 s and multiple scans were used to further improve signal to noise. The degree of complex formation was determined by performing a least-squares fit of the corresponding UV–vis absorption spectrum as a weighted sum of two absorption spectra in the longer-wavelength region (where only the small molecule absorbs), which were the spectrum of 200 μM poly(A) (in nucleotide) and 50 μM small molecule, and the spectrum of free small molecule. For aza4 and berberine, spectra of fully bound ligands could not be obtained even at the highest sample concentration investigated. Therefore, the amount of bound ligand could not be determined by the same two-spectra fitting procedure. As an alternative, for aza4, the ratio of average absorbance between 413 nm and 433 nm (representing bound aza4)

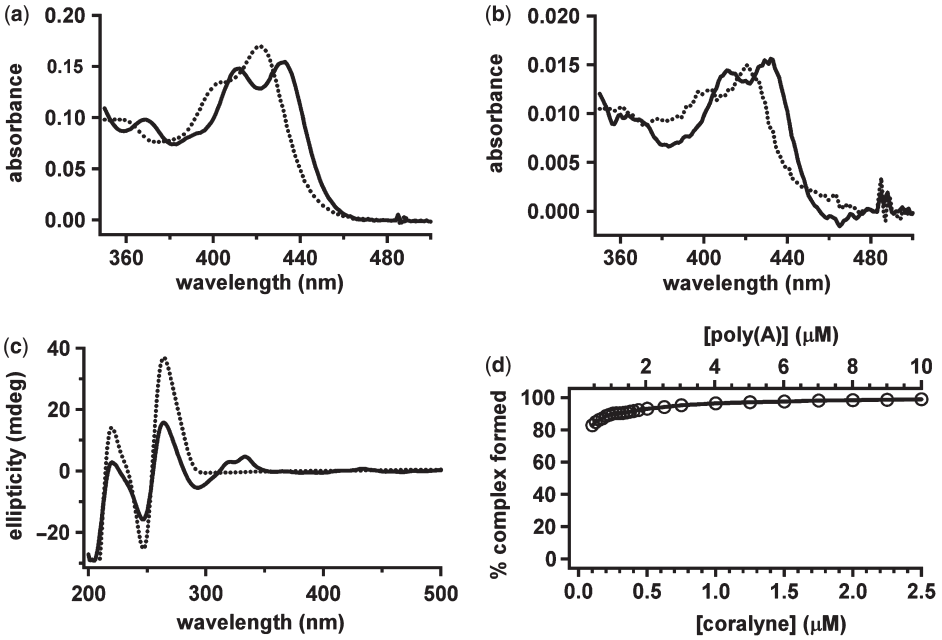

Figure 2. (**a**) Long-wavelength UV–vis spectra of samples containing 1.0 μM coralyne in the presence (solid line) and absence (dashed line) of poly(A), 4 μM in nucleotide. (**b**) Long-wavelength UV–vis spectra of 0.1 μM coralyne in the presence (solid line) and absence (dashed line) of poly(A), 0.4 μM in nucleotide. (**c**) CD spectra of poly(A), 60 μM in nucleotide, in the presence (solid line) and absence (dashed line) of 15 μM coralyne. (**d**) Plot of the percentage of the poly(A)-coralyne complex present as a function of poly(A) and coralyne concentration. Data collected at 22°C. See Materials and Methods section for additional details.

to average absorbance between 339 nm and 359 nm (representing unbound aza4) were plotted with respect to concentration. The spectra were corrected for background using the average absorbance between 437 nm and 457 nm (where the ligand does not absorb). For berberine, the average absorbance from 458–478 nm (bound) relative to 398–418 nm (free) was used after correcting for the background absorbance between 510 nm and 530 nm.

For the poly(A)-aza4 and poly(A)-berberine assemblies, the formalism developed by Kegel and van der Schoot (24) was used to model the number of ligand molecules necessary to form a multimolecular poly(A)-ligand complex. Briefly, for a perfectly cooperative multimolecular-assembly, C_q, that contains q monomers of C_1, the equilibrium equation for assembly can be described by Equation 1.

$$qC_1 \rightleftarrows C_q \qquad \mathbf{1}$$

The fraction of monomers that are incorporated into the assemblies can be written as $f = q[C_q]/C_t$, where $C_t = [C_1] + q[C_q]$. Kegel and van der Schoot have shown that f is a function of q, C_t and the critical micelle concentration, C^*, which is defined as the total concentration of monomers at which half of them are absorbed into assemblies. Specifically,

$$C_t/C^* = f^{1/(q-1)}/\left(2(1-f)^{q/(q-1)}\right) \qquad \mathbf{2}$$

For the poly(A)-aza4 and poly(A)-berberine systems, best fits of dilution data were obtained using Equation 2 when q was set to six or larger.

RESULTS

Coralyne binding to poly(A)

The binding of coralyne to a variety of nucleic acid sequences and structures has been previously reported (28–32). It is well-established that coralyne binds preferentially to DNA triplexes over duplexes, most likely because the shape of coralyne is closer to the shape of a Py·Pu·Py triplet than to a Watson–Crick base pair (29,33). Additionally, we have shown that coralyne assists the template-directed ligation of a triplex in the same way proflavine, a duplex intercalator, assists the template-directed ligation of a duplex (34). A competition dialysis study first established, unexpectedly, that coralyne binds poly(dA) more favorably than Watson–Crick duplex DNA and comparably to triplex DNA (30). Subsequently, our laboratory determined that coralyne binding induces a poly(dA) self-structure that is an antiparallel duplex with a helix that can be incorporated between flanking Watson–Crick duplexes (20). More recently, Xing *et al.* (16) have reported that coralyne binds to poly(A) with a K_a of $1.8 \times 10^6\,M^{-1}$ at pH 7. Here we reexamine the binding of coralyne to poly(A) under similar conditions, but with a different experimental approach.

In Figure 2a, the long-wavelength region is presented from UV–vis absorbance spectra of coralyne in the presence and absence of poly(A). A red shift of ~12 nm is observed upon coralyne binding to poly(A), which is consistent with the π–π stacking of coralyne with the adenine bases, such as that which occurs upon intercalation. The addition of coralyne to poly(A) also results in the

appearance of induced CD bands between 290 nm and 360 nm (Figure 2c). Because coralyne is an achiral molecule, the appearance of induced CD bands confirm the binding of coralyne in the chiral environment of poly(A). Additionally, thermal denaturation, monitored by the change in the intensity of induced CD bands revealed a T_m of 60°C for the poly(A)-coralyne complex, which is consistent with the T_m reported by Xing *et al*. (16).

Dilution experiments, in which buffer is added incrementally to a sample containing a constant ratio of one coralyne molecule per four nucleotides, were conducted to obtain the association constant of the coralyne-poly(A) complex. We have found that maintaining a constant ratio of coralyne:poly(A) by this approach facilitates association constant determination for the primary mode of coralyne binding to poly(A). Previously, it has been shown that the highest affinity mode of coralyne binding to poly(A) is consistent with intercalation of A·A base pairs by coralyne, as the maximum level of binding for this mode obeys the nearest neighbor exclusion principle: one ligand per two base pairs (or four adenine bases in the case of the poly(A) self-structure) (16). We have determined that the poly(A) self-structure can bind additional coralyne molecules by a lower affinity secondary binding mode (e.g. outside helical stacking) (unpublished data). Thus, samples containing higher coralyne:poly(A) ratios can have coralyne associated with poly(A) in a mixture of binding modes, complicating association constant determination. We have also determined that working with lower coralyne:poly(A) ratios than one coralyne per four nucleotides complicates binding studies because the poly(A) self-structure is only stable when a critical number of ligands are bound. Thus, the more standard approach of determining an association constant by measuring a physical observable (e.g. fluorescence) while titrating a ligand into an excess of nucleic acid binding sites can give spurious results if the nucleic acid is not initially in the state that exhibits the binding mode of interest. This latter point is more clearly illustrated by molecules that bind poly(A) with lower affinities than coralyne (vide infra).

For the coralyne-poly(A) dilution experiments, a 200 μM poly(A), 50 μM coralyne sample was diluted incrementally with buffer, and UV–vis absorption spectra were collected after each dilution. This procedure was continued until the sample was too dilute for spectra to be obtained with satisfactory signal-to-noise. A poly(A) concentration of 0.4 μM and a coralyne concentration of 0.1 μM was the lowest measured (Figure 2b). The percentage of the complex formed at each concentration, starting with the highest concentration sample, was determined by fitting each dilution-series spectrum with a two-state model. Briefly, least-squares fits were performed for the 380–480 nm region (a coralyne-only absorption region) of each UV–vis absorption spectrum of the dilution study by a function that was a weighted sum of two absorption spectra: the spectrum of the initial, fully formed coralyne-polynucleotide complex and the spectrum of free coralyne.

The dilution curve obtained using our two-state model exhibited a plateau from the highest sample concentration (i.e. 50 μM coralyne) down to 0.25 μM coralyne (the highest concentration shown in Figure 2b). All spectra were well-fit by the two-state model, and >95% complex formation was observed in this concentration regime. As shown in Figure 2d, the reduced association of coralyne with poly(A) became apparent for samples diluted below 1 μM poly(A), 0.25 μM coralyne, indicating partial secondary structure dissociation. However, even in the case of a sample diluted to 0.4 μM poly(A), 0.1 μM coralyne, ~80% of the poly(A)-coralyne secondary structure is present. A comparison of the spectra for 0.1 μM free coralyne and 0.1 μM coralyne, 0.4 μM poly(A) (Figure 2b) with corresponding spectra for 1 μM free coralyne and 1 μM coralyne, 4 μM poly(A) (Figure 2a) clearly illustrates that the dissociation constant, K_d, of coralyne for the poly(A) self-structure is less than 100 nM. The two-state fits of these spectra, as described above, are provided in Supplementary Data (Figure S1). Dilution spectra obtained for concentrations below 0.1 μM coralyne, 0.4 μM poly(A) were also consistent with an apparent K_a of $>10^7\ M^{-1}$. Signal-to-noise ratios for these samples were not sufficient to more precisely define the apparent association constant.

Ellipticine binding to poly(A)

We have previously demonstrated that proflavine (Figure 3), an intercalator of Watson–Crick duplexes with micromolar affinity, does not bind appreciably to poly(dA) (20). Biver *et al*. (35) have shown some level of proflavine-poly(A) interaction, but the mode of binding

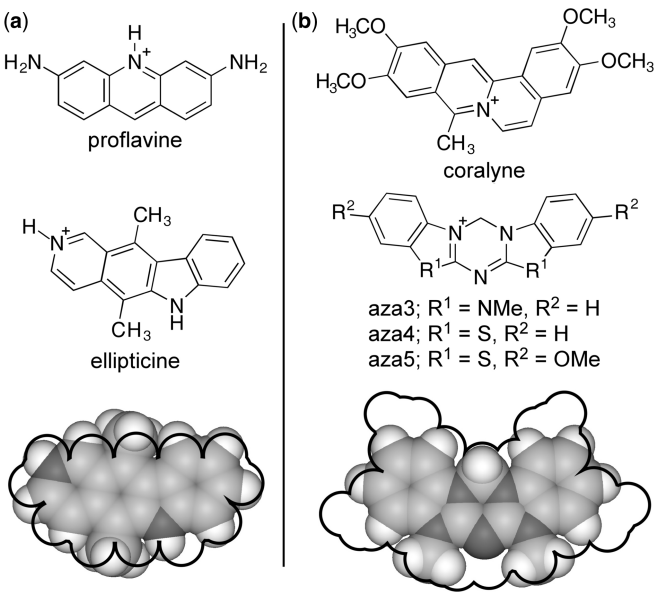

Figure 3. (**a**) Chemical structures of proflavine and ellipticine. Bottom of panel a is a space-filling model of ellipticine overlaid with the outline of a space-filling model of proflavine. (**b**) Chemical structures of coralyne and the azacyanine molecules. Bottom of panel b is a space-filling model of aza3 overlaid with the outline of a space-filling model of coralyne.

does not appear to induce the self-structure at neutral pH. With the goal of discovering additional molecules that bind and stabilize the poly(A) self-structure, we sought to explore ligands that are intermediate in size and shape to coralyne and proflavine. Accordingly, we sought a molecule with a planar ring system that is only minimally larger than proflavine but has a crescent shape. Ellipticine, a molecule known to bind Watson–Crick base pairs, is similar in size to proflavine, but has a crescent shape (Figure 3). We considered this molecule the best initial candidate for this study.

The interactions of ellipticine and its derivatives with DNA have been studied extensively, due to their potential as anticancer drugs (36,37). Ellipticine has been shown by crystallographic studies to bind duplex DNA by intercalation, (38,39) and by fluorescence titration studies to bind calf thymus DNA with an apparent K_a of $10^7\,M^{-1}$ (one of the highest association constants known for a simple intercalator) (40). Competition dialysis has also revealed that ellipticine binds strongly to the hybrid duplex poly(A)·poly(dT), the DNA triplex poly(dA)·poly(dT)$_2$ and the DNA tetraplex formed by d($G_{10}T_4G_{10}$), but not poly(A) (41).

We first investigated the possible binding of ellipticine to poly(A) using both UV–vis and CD spectroscopy. A sample containing one molar equivalent of ellipticine per four nucleotides of poly(A) exhibited a red shift in the longer-wavelength absorption bands, relative to the free ligand (Figure 4a). A weak induced band was also observed in the CD spectrum of the same sample (Figure 4b). Monitoring the change in ellipticity at 296 nm as a function of temperature revealed a T_m of 55°C for the poly(A)-ellipticine complex. A plot of the percentage of poly(A)-ellipticine complex formed as a function of ellipticine/poly(A) concentration, derived from a two-state model (Figure 4c), revealed an apparent K_a of $2 \times 10^5\,M^{-1}$ (K_d, 4.6 μM) for ellipticine binding to poly(A).

Our discovery that ellipticine binds poly(A), although it is smaller than the previously identified molecules that bind the poly(A) self-structure (Figure 1), indicates that the crescent shape of ellipticine and coralyne is a critical feature for binding, as the similar-sized but non-curved proflavine does not bind poly(A) (35). The apparent association constant of ellipticine for poly(A), while comparable to proflavine and ethidium binding to Watson–Crick duplexes, is significantly less than that measured for coralyne binding to poly(A). We hypothesized that a crescent-shaped molecule of intermediate size to ellipticine and coralyne might bind with intermediate affinity.

Azacyanine binding to poly(A)

Azacyanines are a class of planar, bis-benzimidazole analogs that were originally prepared as putative ion channel activators (Figure 3) (25–27). These molecules satisfied our criteria of being crescent-shaped and intermediate in size to ellipticine and coralyne (Figure 3). The ring system of these molecules is very similar in size and shape to coralyne. Therefore, aza3 and aza4, which have no exocyclic groups, are smaller in overall surface area compared to coralyne (Figure 3), as well as the other known poly(A) ligands shown in Figure 1. The azacyanines are also of interest as potential poly(A) ligands because these molecules bind poorly to duplex DNA (42), with an apparent K_a of around 10^3–$10^4\,M^{-1}$.

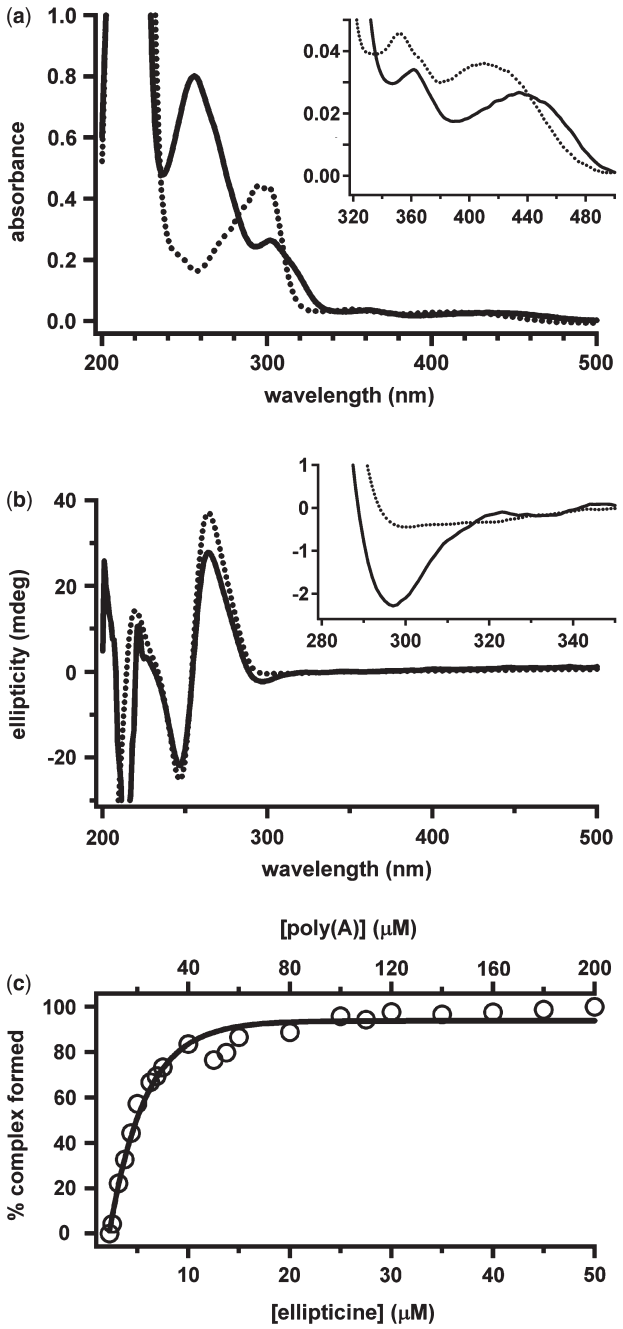

Figure 4. (**a**) UV–vis spectra of ellipticine in the presence (solid line) and absence (dashed line) of poly(A). The inset shows the magnified long-wavelength region. (**b**) CD spectra of poly(A) in the presence (solid line) and absence (dashed line) of ellipticine. The inset shows the magnified long-wavelength region. (**c**) Percentage of poly(A)-ellipticine complex formed as a function of poly(A) and ellipticine concentration with single-exponential fit. Data collected at 22°C. See Materials and Methods section for additional details.

UV–vis spectra of aza3 in the absence and in the presence of poly(A) are shown in Figure 5a. The long-wavelength bands in the UV–vis spectrum of azacyanines are red shifted by ~10 nm in the presence of poly(A), and a hypochromic effect of >25% is also observed (Figure 5a). Both spectral changes are indicative of π–π stacking, which is suggestive of intercalation (43). The induced CD bands observed in the long-wavelength region of the poly(A)-aza3 sample also confirm the binding of azacyanines to poly(A) (Figure 5b). UV–vis and CD spectra of aza4 and aza5 are similar to those shown in Figure 5 for aza3, and both molecules exhibit red shifts, hypochromicity and induced CD bands in the presence of poly(A) (Figure S2).

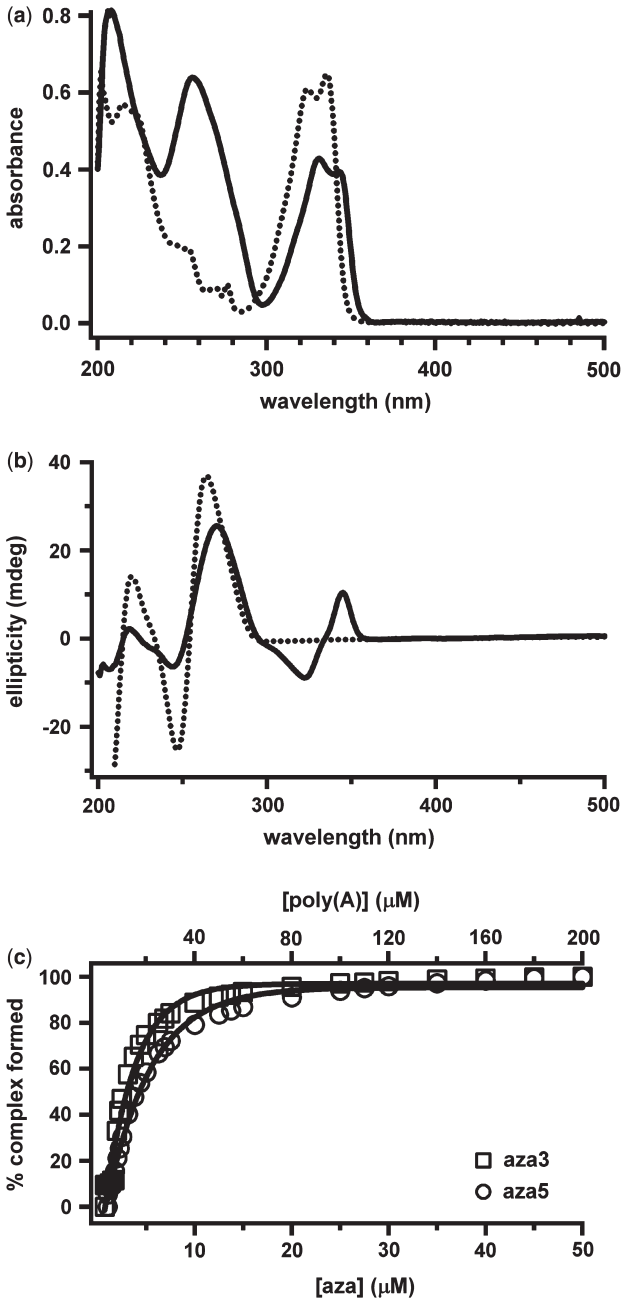

Figure 5. (**a**) UV–vis spectra of aza3 in the presence (solid line) and absence (dashed line) of poly(A), respectively. (**b**) CD spectra of poly(A) with (solid line) and without (dashed line) aza3, respectively. Samples were 60 μM poly(A), 15 μM azacyanine (**c**) Plot of percentage of poly(A)-aza3 and poly(A)-aza5 complex formed as a function of poly(A) and azacyanine concentration with single exponential fits. Data collected at 22°C. See Materials and Methods section for additional details.

CD spectra collected as function of temperature revealed cooperative melting transitions for poly(A) in the presence of aza3 and aza4 with T_ms of 55°C and 30°C, respectively. These cooperative transitions, which are not observed for poly(A) or the azacyanines alone, are consistent with the formation of an azacyanine-induced poly(A) self-structure. It was not possible to obtain an exact T_m for the poly(A) self-structure formed in the presence of aza5, as this molecule decomposed upon heating above 50°C. Nevertheless, the poly(A)-aza5 induced CD band at 40°C was over half as intense as that observed at 5°C, indicating a T_m of >40°C (Figure S3). We found that aza4 also decomposed rapidly above 50°C, but the T_m of the poly(A)-aza4 complex was sufficiently low that a T_m could be determined.

To further investigate the nature of azacyanine binding to poly(A), Job plot analysis was performed (Figure S4). These experiments revealed that azacyanines bind to poly(A) with a stoichiometry of one azacyanine per four nucleotides. The same ligand:poly(A) stoichiometry was previously observed for coralyne binding to poly(dA) and poly(A) (16,28). This binding ratio is again suggestive of intercalative binding, as the poly(A) likely forms an antiparallel duplex, as we demonstrated for poly(dA), and intercalators cannot bind at ratios greater than one ligand per two base pairs in accordance with the nearest-neighbor exclusion principle.

Another distinguishing feature of the coralyne-induced poly(dA) self-structure is that it is destabilized as pH is lowered below neutrality (20). We have investigated the pH-dependent stability of the azacyanine-induced poly(A) self-structure using aza3 as a representative ligand. The aza3-induced poly(A) self-structure is destabilized as the sample pH is lowered below neutrality, as demonstrated by the loss of the induced CD band intensity of aza3 between pH 5.5 and 4.5 (Figure S5). This observation is significant given that poly(A) is known to form a parallel-stranded hemiprotonated self-structure that is most stable around pH 4.5 (44,45). Thus, the pH-dependent stability of the aza3-induced poly(A) self-structure again support this structure as being the same as the coralyne-induced poly(dA) structure.

The dissociation of aza3 and aza5 from poly(A) was monitored by fitting UV–vis spectra with two-state models as described above. The resulting curves revealed apparent association constants of $3.8 \times 10^5\,M^{-1}$ and $2.5 \times 10^5\,M^{-1}$ for aza3 and aza5, respectively (Figure 5). The binding constant of aza4 to poly(A) is discussed in the following section.

Aza4 binding to poly(A)

The analysis used above to determine the association constants of poly(A) ligands utilized two-state models in

which ligand-specific absorption bands of samples containing 50 μM ligand, 200 μM poly(A) were considered representative of 100% ligand bound by poly(A). Support that these samples represent completely complexed ligand and poly(A) was provided by the observation of plateau regions in the dilution curves, which persist down to at least a 10-fold dilution from the most concentrated samples. Additionally, T_m values for each of the ligand-poly(A) complexes discussed above are at least 15°C above room temperature, for samples containing 50 μM ligand, 200 μM poly(A). In contrast, the lack of a plateau region in the aza4 dilution curve indicated that all aza4-poly(A) samples investigated were only partially complexed, even up to a concentration of 50 μM aza4, 200 μM poly(A). This observation was consistent with the T_m of the aza4-poly(A) complex being close to room temperature (i.e. 30°C), for a sample containing 15 μM ligand, 60 μM poly(A). Thus, determination of the association constant of aza4 for poly(A) proved more challenging due to our lack of a sample in which aza4 was fully bound to poly(A).

Despite the additional challenge encountered with determining the association constant of aza4 for poly(A), the dilution curve generated from the most concentrated aza4-poly(A) sample revealed an interesting and informative feature that was not apparent in other ligand-poly(A) dilution curves. In Figure 6 a dilution curve is shown for the aza4-poly(A) sample that was created by plotting the sample absorption ratio A_{423}/A_{349}. This initial step of analysis includes no assumptions regarding whether the most concentrated spectrum represents fully complexed aza4, only that the A_{423}/A_{349} absorption ratio is different for bound and unbound aza4 in the absorption spectrum due to the red shift of aza4 upon binding to poly(A). We note that, unlike the dilution curves presented above, the aza4-poly(A) dilution curve exhibits a cooperative transition between 0 and 25 μM aza4 (Figure 6).

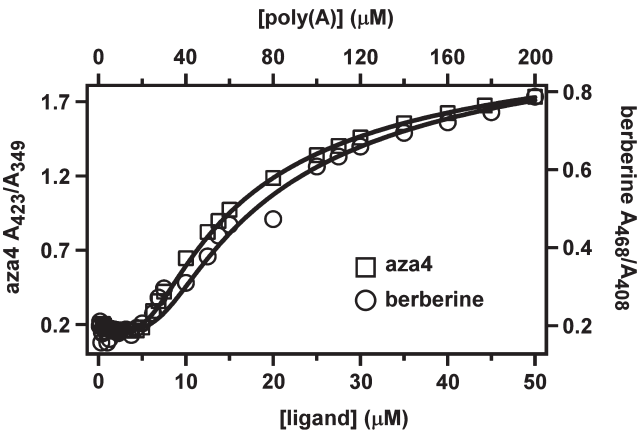

Figure 6. Plots of data obtained from dilution studies of aza4 (open squares) and berberine (open circles) in the presence of poly(A). Both curves are best fits of the micelle-inspired equation (Equation 2) for six ligand molecules being required for stabilization of the poly(A) self-structure. See Materials and Methods section for additional details.

The shape of the aza4-poly(A) dilution curve is reminiscent of curves that monitor the formation of multimolecular assemblies. Micelle formation is a classic example (21–23). The cooperative transition observed in micelle formation as a function of surfactant concentration can be described by the number of surfactants needed to stabilize micelle formation and the concentration at which one half of surfactant molecules are in micelles. This analysis yields what is known as the critical micelle concentration or CMC, below which micelle stability decreases rapidly with surfactant concentration. The concept of the CMC for explaining the behavior of multimolecular assemblies has been successfully applied to a host of other molecular systems, e.g. the assembly of virus capsid proteins (24,46,47).

The aza4-poly(A) dilution data is fit well by the micelle-inspired Equation 2 using three independent parameters: the concentration at which half of the aza4 molecules are bound to poly(A) (i.e. C^*), the number of aza4 molecules needed to stabilize the poly(A) self-structure (i.e. q), and the fraction of complex formed at the highest aza4 concentration. In this fitting procedure the minimum number of aza4 molecules required for complex assembly was restricted to being an integer number. When all three parameters were otherwise allowed to vary independently, the RMS least squares best fit was obtained for half of the aza4-poly(A) complex being formed at an aza4 concentration of 21 μM, a minimum stoichiometery of six aza4 per assembly and a degree of complex assembly at 50 μM aza4 corresponding to 75% bound ligand. Six aza4 molecules could be bound to as few as 24 nt, assuming a loading density similar to that determined for aza3 binding to poly(A). Given that the length of polymers in a poly(A) sample are on the order of hundreds to thousands of nucleotides in length, the six aza4 molecules required for aza4-poly(A) complex formation likely represents the minimum number of molecules necessary to nucleate a complex, with each complex containing far more than six aza4 molecules.

The curve describing the aza4-driven assembly of the poly(A) self-structure is similar to other self-assembling systems (24,48). First, the assembly of poly(A) strands is relatively sharp with respect to poly(A)/aza4 concentration. Second, the highly cooperative nature of the assembly is also apparent by the lack of assembly below a particular concentration (i.e. 5 μM in the case of aza 4). This second feature of the dilution curves illustrates another ligand-specific concentration (in addition to C^*), i.e. the concentration below which a poly(A)-ligand complex is not observed. We refer to this concentration as the minimal concentration required for assembly, or MCA.

Berberine binding to poly(A)

The binding of berberine to poly(A) and poly(dA) has been previously studied by two laboratories. It has recently been reported that berberine binds to poly(A) with a K_a of $3.5 \times 10^5\,M^{-1}$ (at pH 7; 20 mM NaCl, 20°C) as determined by fluorescence titrations (17). However, earlier competition dialysis experiments, with

somewhat different buffer conditions (pH 7; 185 mM NaCl, 20–22°C), revealed no appreciable binding of berberine to poly(dA) (30). Given the fact that the similarly shaped coralyne was able to bind tightly to both poly(A) and poly(dA) and induce self-structure formation, the contrasting results of berberine binding to these nucleic acids reported by two different laboratories was puzzling. Understanding the possible biological targets of berberine is also of interest, as this molecule has been shown to exhibit antisecretory, anti-inflammatory, antibacterial, antimalarial and anticancer activities (49–52).

We have reinvestigated the binding of berberine to poly(A) using the same set of experiments presented above. UV–vis spectra are shown in Figure 7a for berberine in the presence and absence of poly(A). The longest wavelength absorption band of berberine is red shifted and hypochromic in the presence of poly(A). Induced CD bands are observed for berberine in the presence of poly(A) (Figure 7b). Monitoring the ellipticity at 330 nm as a function of temperature revealed a T_m of 30°C.

The dilution curve for berberine in the presence of poly(A) was also generated by plotting an absorption ratio rather than using a two-state model, like aza4, because there was no indication that the sample with the maximum concentration of 50 μM berberine and 200 μM poly(A) was fully assembled. In the case of berberine, the dilution curve was generated using the absorption ratio A_{468}/A_{408} (Figure 6). The resulting curve lacks a plateau and exhibits a cooperative transition with little assembly below ~5 μM berberine (MCA). Given the shape of this curve, the data was also fit by the micelle-inspired Equation 2 (Figure 6). An excellent fit was again obtained with the requirement that at least six berberine molecules be bound for stabilization of the poly(A) self-structure, with half assembly at 25 μM and 71.4% assembly at the highest concentration measured (i.e. 50 μM berberine).

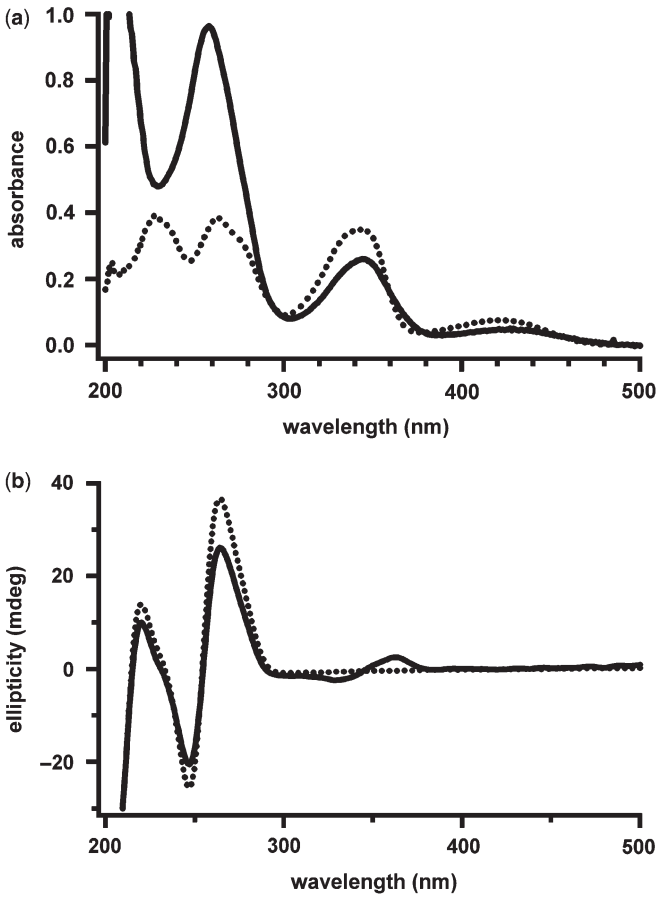

Figure 7. (**a**) UV spectra of berberine in the presence (solid line) and absence (dashed line) of poly(A). (**b**) CD spectra of poly(A) with (solid line) and without (dashed line) berberine, respectively. Samples were 60 μM poly(A), in nucleotide, 15 μM berberine. Data collected at 22°C. See Materials and Methods section for additional details.

DISCUSSION

We have used UV–vis and CD spectroscopy to investigate the association of several small molecules with poly(A). These investigations have confirmed and expanded the set of ligands now known to bind tightly to poly(A) and induce a self-structure at neutral pH. The long-wavelength absorption bands of all molecules investigated exhibit a red shift and significant hypochromism upon binding to poly(A). These spectral changes are indicative of π–π stacking, which is consistent with an intercalative binding mode (43).

The results of the experiments presented here illustrate the importance of the size and shape of molecules that induce formation of the poly(A) self-structure. Here, we have demonstrated that coralyne binds poly(A) with an association constant that is among the highest observed for a simple, planar molecule binding to a nucleic acid duplex (i.e. $K_a > 1 \times 10^7\,M^{-1}$) and the highest reported to date for poly(A). In contrast, berberine, another ligand with a similar shape, but with an extra ring, showed greatly reduced binding (i.e. $K_a < 4 \times 10^4\,M^{-1}$).

These observations motivated us to explore the possibility that molecules smaller than coralyne, but with a similar crescent shape, might also induce the formation of poly(A) self-structure. Ellipticine, a well-known intercalator of Watson–Crick duplexes, was found to bind poly(A) with an apparent association constant of $2 \times 10^5\,M^{-1}$. While interesting with regard to the shape-specificity hypothesis, this molecule is not selective for poly(A) over Watson–Crick duplexes (36).

Three azacyanines were selected for study due to their crescent shape and intermediate size between proflavine and coralyne. The azacyanines also appear promising as a new scaffold for the design of molecules for the binding of poly(A) due to their ease of synthesis and low affinity for Watson–Crick DNA (25,27,42). All three azacyanines were found to bind poly(A), with aza3 and aza5 exhibiting association constants comparable to that of ellipticine. Furthermore, binding data presented here demonstrate the potential to modulate azacyanine binding affinity by making ring substitutions or by the addition of peripheral groups. Specifically, aza4 shows surprisingly reduced binding in comparison to aza3, as a result of the N-methyl to sulfur substitution in the two

five-membered rings. However, aza5, which also contains the sulfur substitutions, exhibits a binding affinity that is 'restored' to that of aza3 by the addition of two methoxy groups at the most distal parts of the molecule. Together, the results presented here illustrate how a specific molecular shape and size range is important for the recognition of poly(A). In addition, comparison of aza3 to aza4, and aza4 to aza5, in binding to poly(A) demonstrates the importance of functional groups and ring substitutions in these molecules for recognition of poly(A).

We have also presented a simple yet effective methodology for obtaining binding constants for ligands of poly(A). For coralyne and berberine this approach has revealed that coralyne binds to poly(A) with an association constant at least 5-fold greater, and berberine binds to poly(A) with an association constant of at least 100-fold lower, when compared to the results from previous studies that were based upon fluorescence titration measurements (16,17). Dilution studies that maintain constant ligand: nucleic acid ratios could prove more reliable in some cases for determining association constants.

The binding of small molecules to poly(A) is clearly different from the binding of small molecules to a pre-structured nucleic acid, such as duplex DNA, where the binding of a ligand molecule can be treated as a single event. In the case of poly(A), small molecule binding and secondary structure formation are coupled events, as the neutral-pH poly(A) self-structure exists only when ligands are bound. Therefore, if the free energy associated with the binding of more than one ligand molecule is necessary to stabilize the poly(A) self-structure, then one should expect a highly cooperative structural transition as a function of ligand concentration. We have shown that by diluting a concentrated poly(A)-small molecule complex, in which the poly(A) is initially in the duplex state, it is possible to determine the minimum number of ligands required for assembly, the C^* (ligand concentration at half assembly), and the concentration below which the ligand-driven poly(A) self-structure does not exist (i.e. the MCA) (Figure 8).

The analysis of molecular systems such as the poly(A)-ligand assemblies by classical drug-DNA binding assays may lead to incomplete or ambiguous results because of the high cooperativity of small molecule binding. For example, a common protocol for determining binding constants by fluorescence is to start with a sample of free ligand molecule (commonly 1 μM) and then to titrate this sample with the nucleic acid (from a solution that also contains 1 μM ligand to maintain constant ligand concentration). The ligand-nucleic acid K_a (or K_d) value is then calculated by fitting the observed changes in fluorescence spectra using a noncooperative model for the binding of the ligand molecule (53). If the K_d of the ligand molecule is approximately equal to or lower than 1 μM (i.e., $K_a \geq 10^6\,M^{-1}$), then the ligand molecules will be bound to poly(A) strands that are assembled into the duplex structure from the first titration point. Therefore, the fluorescence titrations will lack the data points which reflect the onset of ligand binding to poly(A) and the assembly of the poly(A) self-structure. Titration of the nucleic acid only above the MCA may/would show increased binding of the small molecule at higher concentrations, and therefore yield an apparent association constant. However, not appreciating the lack of binding at lower-ligand concentrations (such as observed in aza4 and berberine dilution curves) would not bring to attention the highly cooperative nature of ligand binding. Additionally, the shift of the binding curve to higher nucleic acid concentrations (due to the highly cooperative nature of the assembly) would likely result in the determination of an apparent association constant that is lower than that intrinsic to the cooperative assembly.

In the case of equilibrium dialysis experiments, ligands that induce secondary structure transitions might not be identified even though their association constants are comparable to ligands that bind in a noncooperative manner. More specifically, nucleic acid samples in equilibrium dialysis experiments are brought to equilibrium (across a dialysis membrane) with a putative ligand molecule that is commonly present in the dialysate at a concentration of 1 μM (30). If the K_d of a ligand molecule binding is somewhat higher than 1 μM, and if multiple ligand molecules (q) are needed to stabilize assembly of the nucleic acid secondary structure, there might be no evidence of binding observed. Ellipticine is a good example of such a case. Ellipticine has been shown in the present study to have a K_d for poly(A) of 4.6 μM, but does not show binding by an equilibrium dialysis assay (41), whereas ethidium, which has a similar K_d for duplex DNA, does show binding to duplex DNA in the same assay. We surmise that if

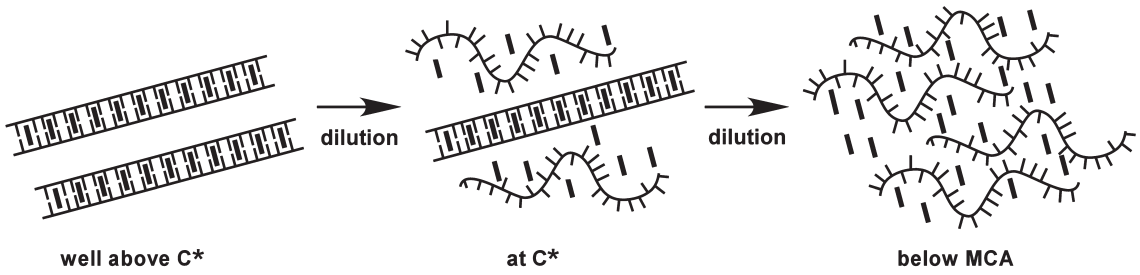

Figure 8. A schematic representation of the disassembly of a poly(A)-small molecule complex by dilution with buffer. At ligand and poly(A) concentrations well above the critical ligand concentration (C^* in Equation 2), poly(A) exists entirely as the ligand-bound duplex. Dilution of the sample to C^* results in release of one half of the ligand molecules and one half of the poly(A) strands become single stranded. Continued dilution below the MCA results in the complete dissociation of poly(A) strands and release of all ligand molecules.

the minimum concentration for assembly (MCA) of ligand binding to an unstructured nucleic acid is higher than the concentration of the ligand in the dialysate, then binding by the ligand will not be observed.

SUPPLEMENTARY DATA

Supplementary Data are available at NAR Online.

ACKNOWLEDGEMENTS

We thank Prof. Roger Wartell and members of the Hud laboratory for helpful discussions and careful reading of the manuscript.

FUNDING

National Science Foundation (CHE0404677); NASA Exobiology Program (NNG04GJ32G). Funding for open access charge: National Science Foundation.

Conflict of interest statement. None declared.

REFERENCES

1. Hurley,L.H. (1989) DNA and associated targets for drug design. *J. Med. Chem.*, **32**, 2027–2033.
2. Mergny,J.L. and Helene,C. (1998) G-quadruplex DNA: a target for drug design. *Nat. Med.*, **4**, 1366–1367.
3. Thurston,D.E. (1999) Nucleic acid targeting: therapeutic strategies for the 21st century. *Br. J. Cancer*, **80**, 65–85.
4. Chaires,J.B. (2005) Structural selectivity of drug-nucleic acid interactions probed by competition dialysis. In Chaires,J.B. and Waring,M.J. (eds), *DNA Binders and Related Subjects*. Vol. 253, Springer, Berlin, pp. 33–53.
5. Ihmels,H. and Otto,D. (2005) Intercalation of organic dye molecules into double-stranded DNA: general principles and recent developments. In Würthner,F. (ed.), *Topics in Current Chemistry: Supramolecular Dye Chemistry,* Vol. 258, Springer, Berlin, pp. 161–204.
6. Palchaudhuri,R. and Hergenrother,P.J. (2007) DNA as a target for anticancer compounds: methods to determine the mode of binding and the mechanism of action. *Curr. Opin. Biotechnol.*, **18**, 497–503.
7. Mao,C., Sun,W., Shen,Z. and Seeman,N.C. (1999) A nanomechanical device based on the B-Z transition of DNA. *Nature*, **397**, 144–146.
8. Yurke,B., Turberfield,A.J., Mills,A.P., Simmel,F.C. and Neumann,J.L. (2000) A DNA-fuelled molecular machine made of DNA. *Nature*, **406**, 605–608.
9. Gothelf,K.V. and LaBean,T.H. (2005) DNA-programmed assembly of nanostructures. *Org. Biomol. Chem.*, **3**, 4023–4037.
10. Park,S.H., Yin,P., Liu,Y., Reif,J.H., LaBean,T.H. and Yan,H. (2005) Programmable DNA self-assemblies for nanoscale organization of ligands and proteins. *Nano Lett.*, **5**, 729–733.
11. Persil,Ö. and Hud,N.V. (2007) Harnessing DNA intercalation. *Trends Biotechnol.*, **25**, 433–436.
12. Wickens,M., Anderson,P. and Jackson,R.J. (1997) Life and death in the cytoplasm: messages from the 3′ end. *Curr. Opin. Genet. Dev.*, **7**, 220–232.
13. Dower,K., Kuperwasser,N., Merrikh,H. and Rosbash,M. (2004) A synthetic A tail rescues yeast nuclear accumulation of a ribozyme-terminated transcript. *RNA*, **10**, 1888–1899.
14. Topalian,S.L., Kaneko,S., Gonzales,M.I., Bond,G.L., Ward,Y. and Manley,J.L. (2001) Identification and functional characterization of neo-poly(A) polymerase, an RNA processing enzyme overexpressed in human tumors. *Mol. Cell Biol.*, **21**, 5614–5623.
15. Topalian,S.L., Gonzales,M.I., Ward,Y., Wang,X. and Wang,R. (2002) Revelation of a cryptic major histocompatibility complex class II-restricted tumor epitope in a novel RNA-processing enzyme. *Cancer Res.*, **62**, 5505–5509.
16. Xing,F., Song,G., Ren,J., Chaires,J.B. and Qu,X. (2005) Molecular recognition of nucleic acids: coralyne binds strongly to poly(A). *FEBS Lett.*, **579**, 5035–5039.
17. Yadav,R.C., Kumar,G.S., Bhadra,K., Giri,P., Sinha,R., Pal,S. and Maiti,M. (2005) Berberine, a strong polyriboadenylic acid binding plant alkaloid: spectroscopic, viscometric, and thermodynamic study. *Biorg. Med. Chem.*, **13**, 165–174.
18. Giri,P., Hossain,M. and Kumar,G.S. (2006) Molecular aspects on the specific interaction of cytotoxic plant alkaloid palmatine to poly(A). *Int. J. Biol. Macromol.*, **39**, 210–221.
19. Giri,P. and Kumar,G.S. (2007) Specific binding and self-structure induction to poly(A) by the cytotoxic plant alkaloid sanguinarine. *Biochim. Biophys. Acta-Gen. Subj.*, **1770**, 1419–1426.
20. Persil,Ö., Santai,C.T., Jain,S.S. and Hud,N.V. (2004) Assembly of an antiparallel homo-adenine DNA duplex by small-molecule binding. *J. Am. Chem. Soc.*, **126**, 8644–8645.
21. Debye,P. (1949) Light scattering in soap solutions. *Ann. N.Y. Acad. Sci.*, **51**, 575–592.
22. Tanford,C. (1980) *The Hydrophobic Effect: Formation of Micelles and Biological Membranes*, 2nd edn., John Wiley & Sons, New York.
23. Ben-Shaul,A. and Gelbart,W.M. (1994) Statistical thermodynamics of amphiphile self-assembly: structure and phase transitions in micellar solutions. In Gelbart,W.M., Ben-Shaul,A. and Roux,D. (eds), *Micelles, Membranes, Microemulsions and Monolayers*, Springer, New York, pp. 1–90.
24. Kegel,W.K. and van der Schoot,P. (2004) Competing hydrophobic and screened-Coulomb interactions in hepatitis B virus capsid assembly. *Biophys J.*, **86**, 3905–3913.
25. Haddadin,M.J., Kurth,J.M. and Olmstead,M.M. (2000) One-step synthesis of new heterocyclic azacyanines. *Tetrahedron Lett.*, **41**, 5613–5616.
26. Galietta,L.J.V., Springsteel,M.F., Eda,M., Niedzinski,E.J., By,K., Haddadin,M.J., Kurth,M.J., Nantz,M.H. and Verkman,A.S. (2001) Novel CFTR chloride channel activators identified by screening of combinatorial libraries based on flavone and benzoquinolizinium lead compounds. *J. Biol. Chem.*, **276**, 19723–19728.
27. Huang,K.S., Haddadin,M.J., Olmstead,M.M. and Kurth,M.J. (2001) Synthesis and reactions of some heterocyclic azacyanines. *J. Org. Chem.*, **66**, 1310–1315.
28. Polak,M. and Hud,N.V. (2002) Complete disproportionation of duplex poly(dT)·poly(dA) into triplex poly(dT)·poly(dA)·poly(dT) and poly(dA) by coralyne. *Nucleic Acids Res.*, **30**, 983–992.
29. MoraruAllen,A.A., Cassidy,S., Alvarez,J.L.A., Fox,K.R., Brown,T. and Lane,A.N. (1997) Coralyne has a preference for intercalation between TA·T triples in intramolecular DNA triple helices. *Nucleic Acids Res.*, **25**, 1890–1896.
30. Ren,J. and Chaires,J.B. (1999) Sequence and structural selectivity of nucleic acid binding ligands. *Biochemistry*, **38**, 16067–16075.
31. Jain,S.S., Polak,M. and Hud,N.V. (2003) Controlling nucleic acid secondary structure by intercalation: effects of DNA strand length on coralyne-driven duplex disproportionation. *Nucleic Acids Res.*, **31**, 4608–4615.
32. Ihmels,H., Faulhaber,K., Vedaldi,D., Dall'Acqua,F. and Viola,G. (2005) Intercalation of oganic dye molecules into double-stranded DNA. Part 2: the annelated quinolizinium ion as a structural motif in DNA intercalators. *Photochem. Photobiol.*, **81**, 1107–1115.
33. Lee,J.S., Latimer,L.J.P. and Hampel,K.J. (1993) Coralyne binds tightly to both T·A·T containing and C·G·C^+ containing DNA triplexes. *Biochemistry*, **32**, 5591–5597.
34. Hud,N.V., Jain,S.S., Li,X. and Lynn,D.G. (2007) Addressing the problems of base pairing and strand cyclization in template-directed synthesis - A case for the utility and necessity of 'molecular midwives' and reversible backbone linkages for the origin of proto-RNA. *Chem. Biodivers.*, **4**, 768–783.
35. Biver,T., Ciatto,C., Secco,F. and Venturini,M. (2006) Dye-induced aggregation of single stranded RNA: a mechanistic approach. *Arch. Biochem. Biophys.*, **452**, 93–101.
36. Garbett,N.C. and Graves,D.E. (2004) Extending nature's leads: the anticancer agent ellipticine. *Curr. Med. Chem. Anti-canc. Agents*, **4**, 149–172.

37. Kohn,K.W., Waring,M.J., Glaubiger,D. and Friedman,C.A. (1975) Intercalative binding of ellipticine to DNA. *Cancer Res.*, **35**, 71–76.
38. Jain,S.C., Bhandary,K.K. and Sobell,H.M. (1979) Visualization of drug-nucleic acid interactions at atomic resolution: 6. structure of two drug-dinucleoside monophosphate crystalline complexes, ellipticine: 5-iodocytidylyl (3′-5′) guanosine and 3,5,6,8-tetramethyl-n-methyl phenanthrolinium-5-iodocytidylyl (3′–5′) guanosine. *J. Mol. Biol.*, **135**, 813–840.
39. Canals,A., Purciolas,M., Aymami,J. and Coll,M. (2005) The anticancer agent ellipticine unwinds DNA by intercalative binding in an orientation parallel to base pairs. *Acta Crystallogr. Sect. D-Biol. Crystallogr.*, **61**, 1009–1012.
40. Müller,W. and Crothers,D.M. (1968) Studies of binding of actinomycin and related compounds to DNA. *J. Mol. Biol.*, **35**, 251–290.
41. Ren,J., Qu,X., Dattagupta,N. and Chaires,J.B. (2001) Molecular recognition of a RNA: DNA hybrid structure. *J. Am. Chem. Soc.*, **123**, 6742–6743.
42. Persil Cetinkol,Ö., Engelhart,A.E., Nanjunda,R.K., Wilson,W.D. and Hud,N.V. (2008) Submicromolar, selective G-quadruplex ligands from one pot: thermodynamic and structural studies of human telomeric DNA binding by azacyanines. *Chembiochem*, **9**, 1889–1892.
43. Bloomfield,V.A., Crothers,D.M. and Tinoco,I. (2000) *Nucleic Acids: Structures, Properties, and Functions*. University Science Books, Sausalito.
44. Rich,A., Davies,D.R., Crick,F.H.C. and Watson,J.D. (1961) The molecular structure of polyadenylic acid. *J. Mol. Biol.*, **3**, 71–86.
45. Maggini,R., Secco,F., Venturini,M. and Diebler,H. (1994) Kinetic study of double-helix formation and double-helix dissociation of polyadenylic acid. *J. Chem. Soc.-Faraday Trans.*, **90**, 2359–2363.
46. Zlotnick,A. (1994) To build a virus capsid: an equilibrium model of the self-assembly of polyhedral protein complexes. *J. Mol. Biol.*, **241**, 59–67.
47. McPherson,A. (2005) Micelle formation and crystallization as paradigms for virus assembly. *Bioessays*, **27**, 447–458.
48. Douglas,J.F., Dudowicz,J. and Freed,K.F. (2008) Lattice model of equilibrium polymerization. VII. Understanding the role of ''cooperativity'' in self-assembly. *J. Chem. Phys.*, **128**, 224901–224917.
49. Kuo,C.L., Chou,C.C. and Yung,B.Y.M. (1995) Berberine complexes with DNA in the berberine induced apoptosis in human leukemic HL-60 cells. *Cancer Lett.*, **93**, 193–200.
50. Ivanovska,N. and Philipov,S. (1996) Study on the anti-inflammatory action of Berberis vulgaris root extract, alkaloid fractions and pure alkaloids. *Int. J. Immunopharmacol.*, **18**, 553–561.
51. Wu,H.L., Hsu,C.Y., Liu,W.H. and Yung,B.Y.M. (1999) Berberine-induced apoptosis of human leukemia HL-60 cells is associated with down-regulation of nucleophosmin/B23 and telomerase activity. *Int. J. Cancer*, **81**, 923–929.
52. Lewis,K. and Ausubel,F.M. (2006) Prospects for plant-derived antibacterials. *Nat. Biotechnol.*, **24**, 1504–1507.
53. Qu,X. and Chaires,J.B. (2000) *Numerical Computer Methods, Part C*. Vol. 321, Academic Press Inc., San Diego, pp. 353–369.